Linear propagation properties for a 300 nm film height Silicon Nitride photonic integration platform in the optical telecom C-band

Luis A. Bru[1], Gloria Micó[1], Daniel Pastor[1], Daniel Pérez[1], David Doménech[2], Ana M. Sánchez[3], Josep M. Cirera[3], Javier Sánchez[3], Carlos Domínguez[3] and Pascual Muñoz[1,2]

[1]*Universitat Politècnica de València - Spain / [2]VLC Photonics - Spain / [3]Institut de Microelectrònica de Barcelona - Centro Nacional de Microelectrónica - Consejo Superior de Investigaciones Científicas - Spain*

pascual@ieee.org

Abstract: In this paper we report on the characterization of the propagation loss, group index, dispersion, birefringence, and thermo-optic phase shift of Si_3N_4 strip waveguides with guiding film height of 300 nm fabricated using low-preassure chemical vapour deposition.

OCIS codes: (130.3120) Integrated optics devices, (220.0220) Optical design and fabrication, (350.2460) Filters, interference.

1. Introduction and state of the art

Si_3N_4 material is widely use in the fabrication of microelectronic circuits, as a support material for developing the devices with other compounds, with whom it exhibits tight electronic, structural and chemical interrelations [1]. For photonics, [2] reports the first fabrication of Si_3N_4 films on SiO_2 buffer on Si wafers, for light propagation in the red visible (VIS) wavelength. A seminal contribution on the application of this material in a functional device was done by [3] with a fully integrated MZI sensor. *Renewed interests* on this material platform started again back in 2005, when [4] and [5] developed processes and demonstrated applications in the near-infrared (NIR). They were followed with SiONx waveguides [6], and later by [7] and [8, 9] with Si_3N_4 waveguides. Up to 2011 demonstrations by telecom related groups are for NIR C-Band at 1550 nm, and all the waveguide cross-sections were for moderate confinement (film heights>100 nm), despite low confinement waveguides (film h<100 nm) [8] were also demonstrated. In 2013, [10] and [11] set new paths of Si_3N_4 technology for visible applications. In parallel, and since 2011, there is a growing interest on high confinement (film h>400 nm) waveguides for the long NIR (wavelength>2000 nm), which are reported by several groups such as [12–15]. For use in the NIR, *low confinement* waveguides were demonstrated with guiding film heights 100 nm, waveguide widths 2800 nm and propagation loss as low as 0.09 dB/cm at 1550 nm for 0.5 mm bend radius. The low propagation loss is due to the low confirment in the Si_3N_4, being most of the mode propagated through the SiO_2, enabled by huge layers of buried and cladding oxide (8 μm). Still for the NIR, *moderate confinement* waveguides (nitride height 150-400 nm) have been demonstrated by several groups. References [4, 16] reported LPCVD Si_3N_4 guiding film heights of 150-200 nm, with waveguide widths 800-2000 nm. The propagation loss reported is 0.11-1.45 dB/cm at 1550 nm for buried oxide (BOX) height up to 5.0 μm. Other groups have reported 3D SiNx on top of SOI in the NIR [17], employing LPCVD Si_3N_4 guiding film heights 300-400 nm, with waveguide widths 800-1000 nm, resulting into propation loss of 1.30-2.10 dB/cm at 1550 nm for BOX heights in between 2.0 and 5.0 μm. Using similar film heights in the VIS and long VIS wavelength ranges, reported PECVD guiding film heights 100-220 nm, waveguide widths 300-800 nm PECVD guiding film loss 0.51-2.25 dB/cm at 532-600 nm for BOX height 2000nm, with increasingly less loss for longer wavelengths (up to 900 nm reported) owing to increased mode confinement. Finally, both for the NIR and long NIR wavelength ranges, *high confinement* waveguides have been reported by [12–15, 18, 19]. Guiding film heights 700-2500 nm, with waveguide widths 700-4000 nm and propagation loss of 0.04-1.37 dB/cm at 1550 nm and 0.16-2.104dB/cm at 2600-3700 nm, for BOX heights in the range of 2.0-8.0 μm have been reported. In the literature, little attention is paid to the full-field propagation properties of moderate film height platforms. *In this paper* we present the characterization of the linear propagation properties, including propagation loss, group index, dispersion, birefringence, thermo-optic phase shift, for Si_3N_4 strip waveguides with guiding film height of 300 nm in the optical telecom C-band.

2. Design, fabrication and characterization

The devices were fabricated on a 100 mm Si wafer, composed of a SiO_2 buffer (2.5 μm thick, n=1.464) grown by thermal oxidation of the silicon substrate, following a LPCVD Si_3N_4 layer with thickness 300nm (n= 2.01) and a

2.0 μm thick SiO_2 (n=1.45) deposited by PECVD. The metal layer stack is 30nm Cr and 100nm Au. In some wafers of the batch, additional process steps were deployed to improve the optical quality of the structures (cf. [4]). A set of test structures, MZIs, spiral waveguides and ring resonators (RRs), Fig. 1, was deployed for strip waveguides of width 1.0 μm. The MZI layout was devised so as to have the length difference only in straight sections of the width of interest, with a bend radius of 50 μm to reduce the footprint. The RRs and spiral waveguides (radius 150 μm for negligible bend loss) were deployed to perform full-field time resolved measurements using optical frequency domain reflectometry (OFDR) [20], in transmission and reflection mode respectively. *Mechanisms responsible of optical loss* in strip silicon nitride waveguides are very well described and experimentally explored, employing different fabrication recipes, by [4]. In short, provided processes are put into place to remove impurities in the silicon nitride and silicon oxide layers (i.e. through annealing), the surface roughness (film roughness and waveguide sidewall roughness) together with the mode confinement at the operation wavelength (given by the waveguide cross-section, width, height, as well by the substrate and cladding heights) are the main factors determining the propagation loss. The propagation loss was derived both from the transmission spectrum of MZIs [21] and the backscattering of spiral waveguides, Fig. 1. Values in the range of 1.2-1.6 dB/cm were obtained for devices in the wafers without oxidation and annealing (in agreement to similar waveguide cross-sections, cf. [7, 17]), so further loss reduction can be expected [4]. From the relative positions of the nulls in the transmission spectra of MZIs, ng=1.90-1.92 was inferred. The dispersion was derived from transmission OFDR measurements of RRs, yielding [-0.7,-1.0] ps/nm·m, that match those from the second derivative of the simulated effective index (-0.75 ps/nm·m). Time resolved OFDR measurements provided the TE and TM propagation delay difference leading to birefringence of 0.168. Finally, thermal tuners of different lengths and widths were characterized, with P_π in [213,270] mW as shown in Fig. 1.

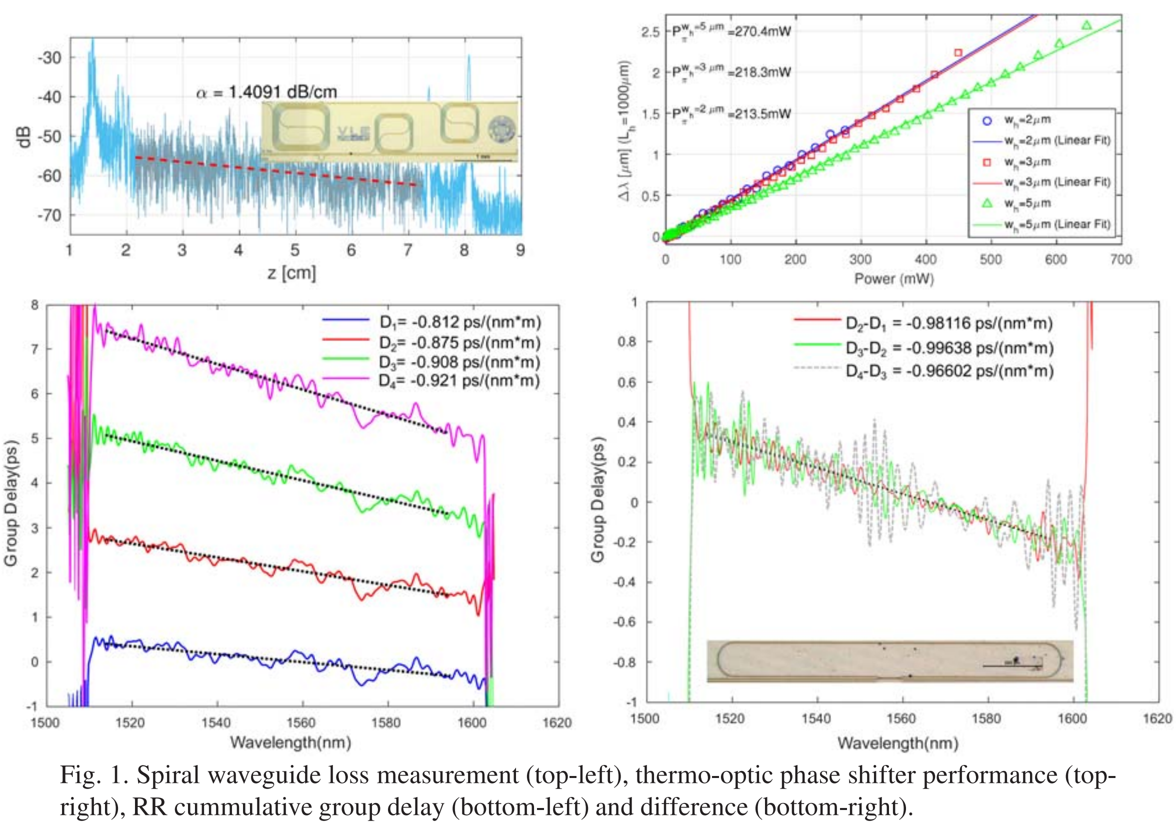

Fig. 1. Spiral waveguide loss measurement (top-left), thermo-optic phase shifter performance (top-right), RR cummulative group delay (bottom-left) and difference (bottom-right).

Acknowledgments

The authors acknowledge financial support through projects TEC2013-42332-P, TEC2015-69787-REDT PIC4TB, TEC2016-80385-P SINXPECT, TEC2014-54449-C3-1-R, GVA PROMETEO 2013/012, EC H2020-ICT-27-2015 CSA 687777 and IP 688519, FEDER UPVOV 10-3E-492 and 08- 3E-008. G.M. acknowledges BES-2014-068523. L.B. acknowledges PTA2015-11309-I.

References

1. E. F. Krimmel and R. Hezel, *Si Silicon: Silicon Nitride in Microelectronics and Solar Cells* (Springer-Verlag Berlin Heidelberg, 1991).
2. W. Stutius and W. Streifer, “Silicon nitride films on silicon for optical waveguides,” Applied Optics **16**, 3218–3222 (1977).
3. E. F. Schipper, A. M. Brugman, C. Dominguez, L. M. Lechuga, R. P. H. Kooyman, and J. Greve, “The realization of an integrated Mach-Zehnder waveguide immunosensor in silicon technology,” Sensors and Actuators B: Chemical **40**, 147–153 (1997).
4. M. J. Shaw, J. Guo, G. A. Vawter, S. Habermehl, and C. T. Sullivan, “Fabrication techniques for low-loss silicon nitride waveguides,” (2005), vol. 5720, pp. 109–118.
5. M. Melchiorri, N. Daldosso, F. Sbrana, L. Pavesi, G. Pucker, C. Kompocholis, P. Bellutti, and A. Lui, “Propagation losses of silicon nitride waveguides in the near-infrared range,” Applied Physics Letters **86**, 121,111+ (2005).
6. K. Worhoff, E. Klein, G. Hussein, and A. Driessen, “Silicon oxynitride based photonics,” in “2008 10th Anniversary International Conference on Transparent Optical Networks,” , vol. 3 (IEEE, 2008), vol. 3, pp. 266–269.
7. S. C. Mao, S. H. Tao, Y. L. Xu, X. W. Sun, M. B. Yu, G. Q. Lo, and D. L. Kwong, “Low propagation loss SiN optical waveguide prepared by optimal low-hydrogen module,” Optics Express **16**, 20,809+ (2008).
8. J. F. Bauters, M. J. R. Heck, D. John, D. Dai, M.-C. Tien, J. S. Barton, A. Leinse, R. G. Heideman, D. J. Blumenthal, and J. E. Bowers, “Ultra-low-loss high-aspect-ratio Si_3N_4 waveguides,” Optics Express **19**, 3163–3174 (2011).
9. J. F. Bauters, M. J. R. Heck, D. D. John, J. S. Barton, C. M. Bruinink, A. Leinse, R. G. Heideman, D. J. Blumenthal, and J. E. Bowers, “Planar waveguides with less than 01 dB/m propagation loss fabricated with wafer bonding,” Optics Express **19**, 24,090–24,101 (2011).
10. S. Romero-García, F. Merget, F. Zhong, H. Finkelstein, and J. Witzens, “Silicon nitride CMOS-compatible platform for integrated photonics applications at visible wavelengths,” Optics Express **21**, 14,036–14,046 (2013).
11. A. Z. Subramanian, P. Neutens, A. Dhakal, R. Jansen, T. Claes, X. Rottenberg, F. Peyskens, S. Selvaraja, P. Helin, B. Du Bois, K. Leyssens, S. Severi, P. Deshpande, R. Baets, and P. Van Dorpe, “Low-Loss Singlemode PECVD Silicon Nitride Photonic Wire Waveguides for 532–900 nm Wavelength Window Fabricated Within a CMOS Pilot Line,” IEEE Photonics Journal **5**, 2202,809 (2013).
12. T. J. Kippenberg, R. Holzwarth, and S. A. Diddams, “Microresonator-Based Optical Frequency Combs,” Science **332**, 555–559 (2011).
13. K. Luke, Y. Okawachi, M. R. E. Lamont, A. L. Gaeta, and M. Lipson, “Broadband mid-infrared frequency comb generation in a Si_3N_4 microresonator,” Optics Letters **40**, 4823+ (2015).
14. C. J. Krückel, A. Fülöp, T. Klintberg, J. Bengtsson, P. A. Andrekson, and V. Torres-Company, “Linear and nonlinear characterization of low-stress high-confinement silicon-rich nitride waveguides,” Optics Express **23**, 25,827+ (2015).
15. K. Luke, A. Dutt, C. B. Poitras, and M. Lipson, “Overcoming Si_3N_4 film stress limitations for high quality factor ring resonators,” Optics Express **21**, 22,829–22,833 (2013).
16. K. Shang, S. Pathak, B. Guan, G. Liu, and S. J. B. Yoo, “Low-loss compact multilayer silicon nitride platform for 3D photonic integrated circuits,” Optics Express **23**, 21,334+ (2015).
17. W. D. Sacher, Y. Huang, G.-Q. Lo, and J. K. S. Poon, “Multilayer Silicon Nitride-on-Silicon Integrated Photonic Platforms and Devices,” Journal of Lightwave Technology **33**, 901–910 (2015).
18. P. T. Lin, V. Singh, L. Kimerling, and A. M. Agarwal, “Planar silicon nitride mid-infrared devices,” Applied Physics Letters **102**, 251,121+ (2013).
19. J. P. Epping, M. Hoekman, R. Mateman, A. Leinse, R. G. Heideman, A. van Rees, P. J. M. van der Slot, C. J. Lee, and K.-J. Boller, “High confinement, high yield Si_3N_4 waveguides for nonlinear optical applications,” Optics Express **23**, 642+ (2015).
20. U. Glombitza and E. Brinkmeyer, “Coherent frequency-domain reflectometry for characterization of single-mode integrated-optical waveguides,” Journal of Lightwave Technology **11**, 1377–1384 (1993).
21. M. A. Tran, T. Komljenovic, J. C. Hulme, M. L. Davenport, and J. E. Bowers, “A robust method for characterization of optical waveguides and couplers,” IEEE Photonics Technology Letters **28**, 1517–1520 (2016).